Inelastic Behavior of Perforated Plates Subjected to Bending

K. Nakamura, M. Takenaka

Takasago Technical Institute, Mitsubishi Heavy Industries, Ltd., 2-1-1, Shinhama, Arai-cho, Takasago, Hyogo 676, Japan

T. Muto

Power Reactor and Nuclear Fuel Development Corporation, 9-13, 1-chome, Akasaka, Minato-ku, Tokyo 107, Japan

Summary

Inelastic analysis may be required to evaluate the behavior of perforated plates used at elevated temperature such as steam generator tube sheets of fast breeder reactors. We have presented in previous papers a method of inelastic analysis utilizing the concept of the equivalent solid plate, where the inelastic material constants of the equivalent solid plate are determined on the basis of the inelastic behavior of the perforated plate subjected to in-plane loadings. The applicability of the method to the case of out-of-plane loading was still to be examined. In order to investigate into this problem, we have performed experiments to measure the elastic-plastic-creep responses of perforated plates when subjected to four point bending and compared them with the calculated results utilizing the concept of the equivalent solid plate.

Twelve test plates were made of type 304 stainless steel, each 38 mm high, about 90 mm wide and 1000 mm long and had a perforated region with a uniform triangular penetration pattern having a ligament efficiency of 0.3 or 0.5 in the central part of about 300 mm length. The distance between the support points was 900 mm and that between the loading points was 500 mm.

The tests are classified into three groups:

(1) Elastic-plastic tests at room temperature

(2) Elastic-plastic-creep tests at 600°C

(3) Relaxation test at 600°C

The inelastic analysis of perforated plates consists of two steps:

(A) Analysis of the perforated unit cell subjected to in-plane loading to extract the inelastic properties of the equivalent solid plates

(B) Analysis of the equivalent solid plate subjected to four point bending

In the analysis (A), the Ludwik type stress-strain curve and Norton-Bailey's creep law were assumed for the material. It was shown that the equivalent solid plate then obeys approximately the same constitutive equations with modified constants depending upon the ligament efficiency.

The comparison of the experimental results with the results of analysis (B) showed:

(i) The accuracy of the elastic-plastic analysis of the perforated plates was within 20% in terms of the center deflection, which indicates the applicability of the equivalent solid plate defined by in-plane loading behaviors to bending problems.

(ii) Deflections due to creep may be obtained just as well if one uses such creep constants of the material that describe bending creep behavior adequately. Hence the equivalent solid plate determined by in-plane loading is also applicable to bending creep problems.

1. Introduction

The inelastic behaviors of the perforated plates have been investigated by Slot and Branca [1], Porowski and O'Donnell [2] and the authors [3]. The concept of the equivalent solid plate is used in these studies. The inelastic material properties of the equivalent solid plate are determined from the response of the unit cell of the perforated plate subjected to in-plane loadings. The applicability of these properties of the equivalent solid plate to out-of-plane bending problems, which are practically important, must be verified by the experiments.

This paper describes the experimental and calculated results of the perforated plates when subjected to four point bending.

2. Test Material

The material used in this experiment was JIS SUS304 (equivalent to AISI 304) austenitic stainless steel supplied as rolled 40mm thick, 2000mm wide, 1000mm long plate. The chemical composition in weight percentage is given in Table I. This plate had been annealed at 1100°C for 48 minutes and water quenched. All perforated plates were machined to allow the longitudinal direction parallel to the rolling direction of the plate. Then they were reannealed at 1080°C for 40 minutes and water quenched to relieve residual stress and work hardening resulted from drilling.

The tensile properties at room temperature and 600°C are shown in Table II.

3. Experimental Procedure

Perforated plates used for four point bending tests are shown in Fig. 1. Perforated plates are classified into four types according to the hole arrangement and the ligament efficiency. The holes of type A and type C perforated plates are in an array of equilateral triangles one side of which is parallel to the longitudinal direction of the perforated plate. This hole arrangement is called here X-direction. The holes of type B and type D perforated plates are in an array of equilateral triangles one side of which is perpendicular to the longitudinal direction of the perforated plate. This hole arrangement is called here Y-direction. The ligament efficiency η is defined by

$$\eta = h/P$$

where h is the width of ligament at the minimum cross section and P is the distance between hole center lines. Type A and type B perforated plates have a ligament efficiency of 0.3. Type C and type D perforated plates have a ligament efficiency of 0.5. The photograph of the four types of the perforated plates are shown in Fig. 2.

The electro-hydraulic four point bending tester manufactured by MTS Systems Corporation with half of its furnace removed is shown in Fig. 3. The distance between loading points is 500mm and the distance between support points is 900mm. The deflections of the specimen is detected by the displacement gages under the furnace using crystal bars.

The loading conditions for the four point bending tests of perforated plates are listed in Table III. Twelve perforated plates were tested; four perforated plates for plastic tests at room temperature, four for creep tests at 600°C and four for relaxation tests at 600°C. Constant load F is applied at two loading points during the creep test. Constant displacement δ is held at two loading points during the relaxation test.

4. Inelastic Analysis Method

The inelastic finite element analysis of the perforated plates utilizing the concept of the equivalent solid plate consists of the following steps:

(A1) Analysis of the perforated unit cell subjected to in-plane loading to obtain the stress-strain curve of the equivalent solid plate

(A2) Analysis of the perforated unit cell subjected to in-plane constant load to obtain the creep curve of the equivalent solid plate

(B) Analysis of the equivalent solid plate subjected to four point bending

The inelastic finite element program used in this study is MARC program developed by MARC Analysis Research Corporation. In the elastic-plastic analysis the von Mises' yield criterion, the associated flow rule and the Ludwik type stress-strain representation are used as the constitutive equations. In the creep analysis the associated flow rule, the total creep strain hardening law and the Norton-Bailey's creep law are used as the constitutive equations.

The perforated cell used in the analyses (A1) and (A2) is shown in Fig. 4. The element used in this figure is the plane stress quadrilateral element. The method of the analyses (A1) and (A2) is almost the same as that of the previous paper [3] except for the stress-strain relation and the creep strain representation. Refer to the previous paper [3] for the details of the analyses (A1) and (A2). For example, the stress-strain curve of the equivalent solid plate in the direction of the x axis is obtained by calculating the response of the perforated cell when the edge QR is pulled in the direction of the x axis. The Ludwik type stress-strain relation is used for the material to represent the behavior of the type 304 stainless steel well:

$$\begin{cases} \varepsilon = \dfrac{\sigma}{E} & \text{for } \sigma \leq \sigma p, \quad (1) \\ \varepsilon = \dfrac{\sigma}{E} + \left(\dfrac{\sigma - \sigma p}{K}\right)^{\frac{1}{m}} & \text{for } \sigma > \sigma p, \quad (2) \end{cases}$$

where ε is the elastic strain plus plastic strain, σ is the stress, σp is the proportional limit, E is Young's modulus and m and K are the material constants. The stress-strain relation of the equivalent solid plate is also represented by the Ludwik type equations (1) and (2). The proportional limit $\sigma_p{}^*$ is the effective stress when initial local yielding begins at the hole boundary. The coefficient m* and K* are determined by the following equations:

$$m^* = \frac{\log\left(\dfrac{\sigma_i{}^* - \sigma p^*}{\sigma y^* - \sigma p^*}\right)}{\log\left(\dfrac{\varepsilon_i{}^* - \sigma_i{}^*/E}{0.002}\right)} \tag{3}$$

$$K^* = \frac{\sigma y^* - \sigma p^*}{0.002^{m^*}} \tag{4}$$

where $\sigma_i{}^*$ is the effective stress when the effective strain is $\varepsilon_i{}^*$, $\varepsilon_i{}^* = 0.02$ is used here and $\varepsilon_y{}^*$ is the 0.2% offset yield stress for the equivalent solid plate determined from the calculated effective stress-strain curve of the perforated cell according to the ordinary procedure.

The creep curve of the equivalent solid plate in the direction of the x axis is obtained by calculating the time dependent response when the edge QR of the perforated cell is pulled in the direction of the x axis to the value to produce a prescribed effective stress and held for a desired time. The Norton-Baily's creep law is used for the material:

$$\varepsilon^c = A \sigma^n t^s \tag{5}$$

where ε^c is the creep strain, t is the time and A, n, s are the material constants. The creep curves of the equivalent solid plate are also represented by the Norton-Baily's equation (5). The creep coefficients A*, n*, s* for each equivalent solid plate are determined from the three creep curves for the effective stresses, $\sigma_p{}^*$, $2\sigma_p{}^*$ and $3\sigma_p{}^*$ using the least squares method.

The element used in the analysis of the equivalent solid plate subjected to four point bending is the ordinary beam-column element. The material properties of the equivalent solid plate obtained in the analyses (A1) and (A2) are used for the perforated part of the test plate. The original material properties are used for the non-perforated part of the test plate.

5. Results

5-1 Results of Experiments

The results of the experiments are represented in terms of the response of the average loads and center deflections, which typify the overall structural response.

The results of the perforated plates 1 through 4 are shown in Fig. 5. The ordinate is the average load of the two lateral loads and the abscissa is the center deflection. While the perforated plates 1 and 2 show the same responses in the elastic region, those show the different responses in the plastic region. This is because the perforated plate is anisotropic in the plastic region. The "Y-directioned" perforated plate 2 is harder than the "X-directioned" perforated plate 1.

The results of the perforated plates 5 through 8 are shown in Fig. 6.

The results of the perforated plates 9 through 12 are shown in Fig. 7.

5-2 Properties of Equivalent Solid Plate

The stress-strain curves of the equivalent solid plate are shown in Fig. 8. The coefficients of Ludwik equation (2) are determined from these curves and listed in Table IV.

The creep curves for the type A equivalent solid plate (X-direction, $\eta = 0.3$) is shown in Fig. 9. The ordinate is the effective creep strain ϵ^{c*} and the abscissa is the time. The stress levels are the proportional limit σ_p^*, $2\sigma_p^*$ and $3\sigma_p^*$. The coefficients of Norton-Baily's rule are determined by the least squares method and listed in Table V. The solid line and broken lines in Fig. 9 are those of Norton-Baily's rule for three stress levels. All symbols are fairly on the solid line or the broken lines. Results of the perforated plate of the other types are the same. The creep curve of the equivalent solid plates is also able to be represented by Norton-Bailey's rule.

5-3 Comparison of Calculated Results with Measured Results

Typical elastic-plastic response of the perforated plate subjected to four point bending is shown in Fig. 10. The open symbols are the measured results and the solid symbols are the calculated results. The circles indicate the center deflections and the triangles indicate the loading point deflections. The calculated results agree with the experimental results. The accuracy of the elastic-plastic analysis of the perforated plates is listed in Table VI. The accuracy is within 20% except two data at room temperature. These exceptions are mainly due to "cold creep". The loads of the perforated plates 1 through 4 are applied stepwise under manual control while the loads of the other perforated plates are applied in proportion to time under program control for 30 seconds. The deflection of the perforated plates 1 through 4 increased in the plastic region while the loads are held constant for a few minutes. This is the creep phenomenon of type 304 stainless steel at room temperature and called "cold creep".

The comparison of the measured and the calculated time-dependent response for the perforated plate 5 at 600°C is shown in Fig. 11. The circles indicate the experimental results. The normal triangles indicate the calculated results by the inelastic finite element method. The calculation overestimates the creep deformation of the perforated plate. The accuracy of the creep analysis is listed in Table VII. ΔD is the increment of the center deflection after the load reaches the prescribed value. The ratio of the calculated ΔD to the measured ΔD are from 3.4 to 4.6 for the perforated plates. That of the solid beam is 2.6. The solid beam is 40mm high, 37mm wide and 1000mm long. The test procedure is the same as the perforated plates. The calculation overestimates the creep deformation of the solid beam. This means that the creep coefficients for the material listed in Table V are not appropriate. This is because these coefficients are calculated from 13 uniaxial creep data tested at relatively high stresses of $8\ \mathrm{kgf\cdot mm^{-2}}$ to $24\ \mathrm{kgf\cdot mm^{-2}}$. If the modified creep coefficient A^*

$$A^* = 0.3A = 0.666 \times 10^{-8}$$

is used in place of A, the accuracy of the solid plate is 0.93 and that of the perforated plate 5 is 1.22.

6. Conclusion

The elastic-plastic-creep behaviors of the perforated plates when subjected to four point bending at room temperature and 600°C are measured and analyzed by the inelastic finite element method utilizing the concept of the equivalent solid plate. The comparison of the experimental results with the calculated results brought the following conclusion: The equivalent solid palte defined by in-plane loading behaviors is also applicable to the inelastic bending problems.

References

[1] Slot, T. and Branca, T.R., "On the Determination of Effective Elastic-Plastic Properties for the Equivalent Solid Plate Analysis of Tube Sheets", Journal of Pressure Vessel Technology, Transactions of the ASME, August 1974, pp. 220 – 227.

[2] Porowski, J.S. and O'Donnell, W.J., "Plastic Strain Concentrations in Ligaments", Journal of Pressure Vessel Technology, Transactions of the ASME, May 1977, pp. 328 – 336.

[3] Uragami, K., Nakamura, K., Asada, K. and Kano, T., "Inelastic Analysis of Perforated Plates Using Equivalent Solid Plates", Paper No. L12/1, 6th SMiRT, 1981.

Table I Chemical Composition in Weight Percentage

C	Si	Mn	P	S	Ni	Cr	Co	Fe
0.05	0.58	1.00	0.028	0.007	9.10	18.45	0.07	balance

Table II Tensile Properties

Temperature (°C)	0.2% Offset Yield Stress ($kgf \cdot mm^{-2}$)	Tensile Strength ($kgf \cdot mm^{-2}$)	Fracture Elongation (%)	Reduction of Area (%)
25	22.4	68.1	59	77
600	12.3	34.3	40	72

Table III Loading Conditions for Four Point Bending Tests of Perforated Plates

Number	Inelastic Behavior	Temperature	Perforated Plate			Load or Displacement	Hold Time
			Type	Ligament Efficiency η	Direction		
1	Plastic	R.T.	A	0.3	X	–	–
2	Plastic	R.T.	B	0.3	Y	–	–
3	Plastic	R.T.	C	0.5	X	–	–
4	Plastic	R.T.	D	0.5	Y	–	–
5	Creep	600°C	A	0.3	X	F = 300 kgf	300 h
6	Creep	600°C	B	0.3	Y	F = 600 kgf	300 h
7	Creep	600°C	C	0.5	X	F = 600 kgf	300 h
8	Creep	600°C	D	0.5	Y	F = 800 kgf	300 h
9	Relaxation	600°C	A	0.3	X	δ = 5 mm	50 h
10	Relaxation	600°C	B	0.3	Y	δ = 7 mm	50 h
11	Relaxation	600°C	C	0.5	X	δ = 7 mm	50 h
12	Relaxation	600°C	D	0.5	Y	δ = 7 mm	50 h

Table IV Stress-Strain Relations for Material and Equivalent Solid Plates

Perforated Plate	Temp.	Direction	Ligament Efficiency η	Young's Modulus E kgf·mm^{-2}	E^*/E	Poisson's Ratio ν	σ_p kgf·mm^{-2}	σ_y kgf·mm^{-2}	K kgf·mm^{-2}	m	1/m	Type
Material	R.T.	–	–	19000	–	0.264	13.33	21.00	43.05	0.2800	3.5584	–
Material	600°C	–	–	15200	–	0.310	6.870	11.30	33.57	0.3259	3.0085	–
1	R.T.	X	0.3	5344	0.2699	0.371	1.769	5.505	12.20	0.1870	5.3474	A
2	R.T.	Y	0.3	5345	0.2690	0.371	2.885	7.140	14.03	0.1921	5.2065	B
3	R.T.	X	0.5	10523	0.5315	0.299	3.090	10.14	22.29	0.1853	5.3960	C
4	R.T.	Y	0.5	10524	0.5315	0.299	3.912	12.37	24.68	0.1724	5.8013	D
5, 9	600°C	X	0.3	4103	0.2699	0.384	0.913	3.030	8.380	0.2214	4.5174	A
6, 10	600°C	Y	0.3	4103	0.2700	0.384	1.487	3.852	9.993	0.2319	4.3120	B
7, 11	600°C	X	0.5	8079	0.5315	0.323	1.593	5.500	15.63	0.2232	4.4811	C
8, 12	600°C	Y	0.5	8077	0.5314	0.323	2.016	6.050	17.17	0.2108	4.7440	D

Note :

$$\begin{cases} \varepsilon = \dfrac{\sigma}{E} & \text{for} \quad \sigma \leq \sigma_p \\ \varepsilon = \dfrac{\sigma}{E} + \left(\dfrac{\sigma - \sigma_p}{K}\right) & \text{for} \quad \sigma \leq \sigma_p \end{cases}$$

Table V Creep Properties for Material and Equivalent Solid Plates at 600°C

Type	Direction	Ligament Efficiency η	A	n	s
Material	–	–	2.2184×10^{-8}	4.0634	0.60111
A	X	0.3	7.0753×10^{-6}	3.7319	0.56756
B	Y	0.3	2.1477×10^{-6}	4.0405	0.57117
C	X	0.5	3.8202×10^{-7}	4.1656	0.62620
D	Y	0.5	2.3421×10^{-7}	4.0745	0.63127

Note o Norton-Bailey's Rule o Unit

$$\varepsilon^c = A\sigma^n t^s$$

ε^c : mm/mm
σ : kgf·mm^{-2}
t : h

Table VI Accuracy of Elasto-Plastic Analysis of Perforated Plates Subjected to Four Point Bending

Inelastic Behavior	Perforated Plate	Type	Direction	Ligament Efficiency η	Temperature	Load or Displacement	Experiment: Load F_{exp} kgf	Experiment: Cent. Defl. D_{exp} mm	FEM Analysis: Load F_{calc} kgf	FEM Analysis: Cent. Defl. D_{calc} mm	Accuracy: F_{calc}/F_{exp}	Accuracy: D_{calc}/D_{exp}
Plastic	1	A	X	0.3	R.T.	F = 940 kgf	940	18.30	940	17.2	1.00	0.94
	2	B	Y	0.3	R.T.	F = 1000 kgf	1000	15.70	1000	10.3	1.00	0.66
	3	C	X	0.5	R.T.	F = 1700 kgf	1700	16.20	1700	17.0	1.00	1.05
	4	D	Y	0.5	R.T.	F = 1000 kgf	1000	16.20	1800	11.8	1.00	0.73
Creep	5	A	X	0.3	600°C	F = 360 kgf	360	3.45	360	4.14	1.00	1.20
	6	B	Y	0.3	600°C	F = 600 kgf	595	13.90	600	13.38	1.01	0.66
	7	C	X	0.5	600°C	F = 600 kgf	604	4.10	600	3.53	0.99	0.86
	8	D	Y	0.5	600°C	F = 800 kgf	798	5.90	800	5.42	1.00	0.92
Relaxation	9	A	X	0.3	600°C	δ = 5 mm	470	9.00	455	8.93	0.97	0.90
	10	B	Y	0.3	600°C	δ = 7 mm	561	12.50	591	12.54	1.05	1.00
	11	C	X	0.5	600°C	δ = 7 mm	967	11.60	887	12.34	0.92	1.06
	12	D	Y	0.5	600°C	δ = 7 mm	963	12.05	1016	12.22	1.06	1.01

Table VII Accuracy of Creep Analysis of Perforated Plates Subjected to Four Point Bending at 600°C

Creep Coefficient A'	Perforated Plate	Type	Direction	Ligament Efficiency η	Load	Hold Time	Defl. due to Creep ΔD: ΔD_{exp} mm	Defl. due to Creep ΔD: ΔD_{calc} mm	Accuracy $\Delta D_{calc}/\Delta D_{exp}$
A' = A)	5	A	X	0.3	F = 360 kgf	300 h	4.1	16.05	3.92
	6	B	Y	0.3	F = 600 kgf	300 h	16.9	56.95	3.37
	7	C	X	0.5	F = 600 kgf	300 h	4.1	14.52	3.54
	8	D	Y	0.5	F = 800 kgf	300 h	6.6	30.65	4.64
	Solid Beam	–	–	–	F = 600 kgf	100 h	4.45	13.02	2.93
A' = 0.3A	5	A	X	0.3	F = 360 kgf	300 h	4.1	4.99	1.22
	Solid Beam	–	–	–	F = 600 kgf	100 h	4.45	4.14	0.93

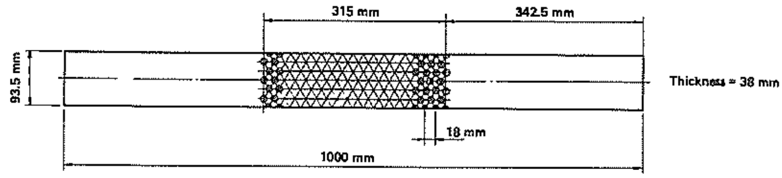

(1) X-direction: Type A (Hole Diameter = 12.6 mm) or Type C (Hole Diameter = 9 mm)

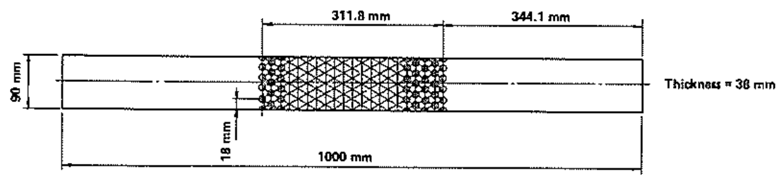

(2) Y-direction: Type B (Hole Diameter = 12.6 mm) or Type D (Hole Diameter = 9 mm)

Fig. 1 Perforated Plates

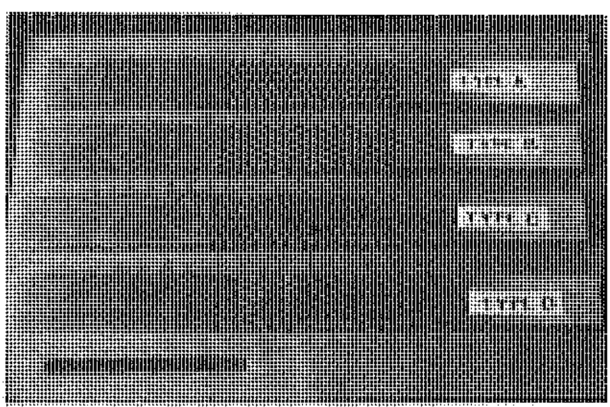

Fig. 2 Four Types of Perforated Plates

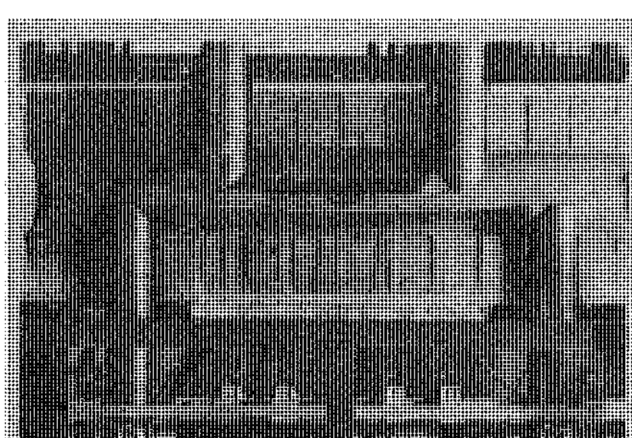

Fig. 3 Four Point Bending Tester

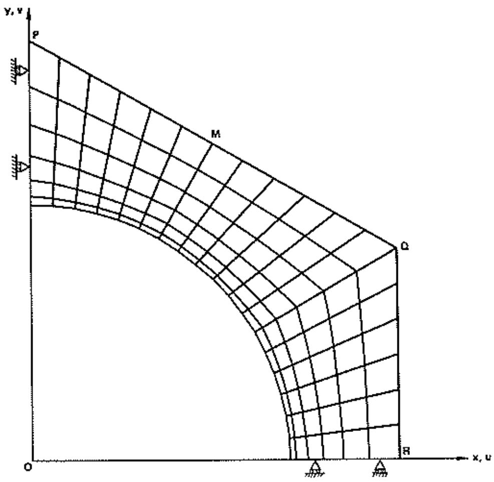

Fig. 4 Perforated Cell

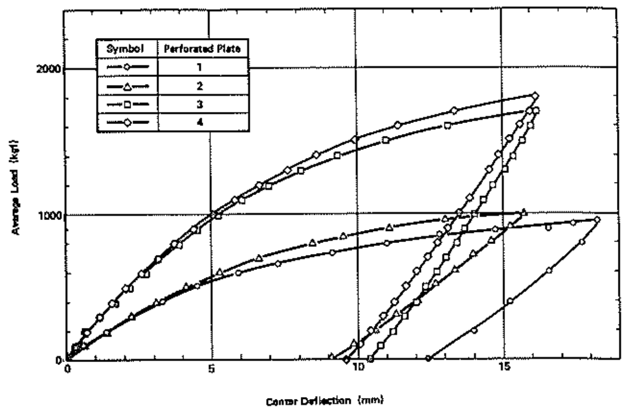

Fig. 5 Load versus Center Deflection for Perforated Plates 1–4 at Room Temperature

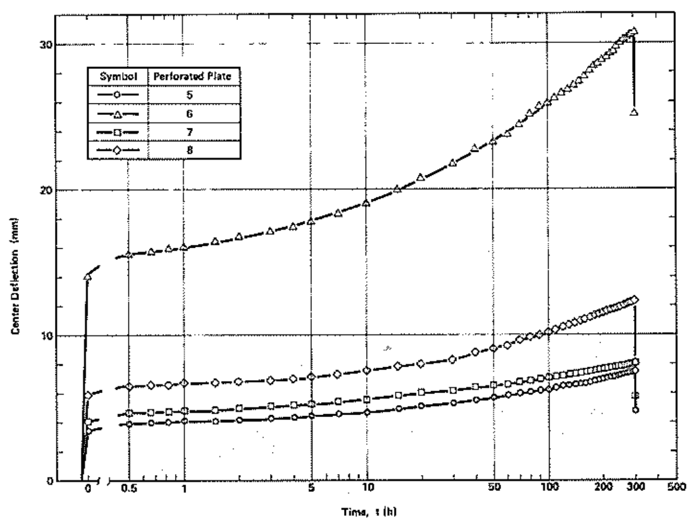

Fig. 6 Center Deflection versus Time for Perforated Plates 5–8 at 600°C

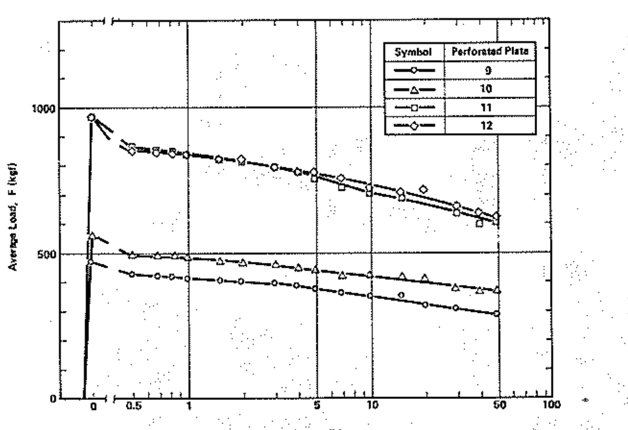

Fig. 7 Load Relaxation versus Time for Perforated Plates 9–12 at 600°C

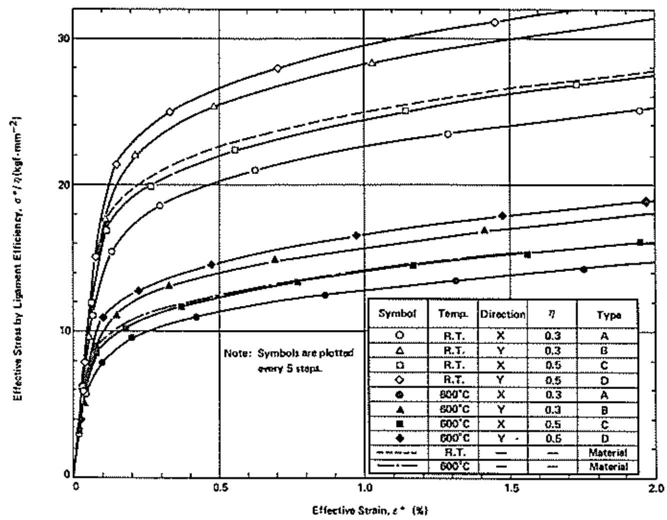

Fig. 8 Stress-Strain Curves for Equivalent Solid Plates

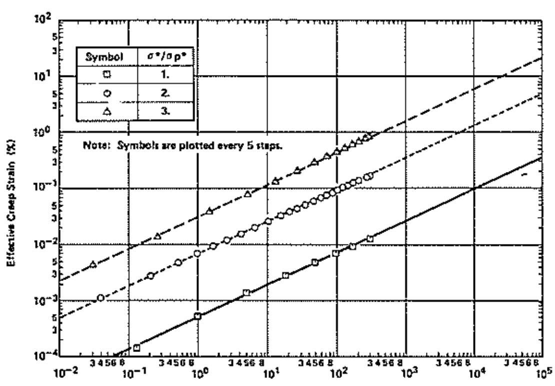

Fig. 9 Creep Curves for Equivalent Solid Plate (Type A) at 600°C

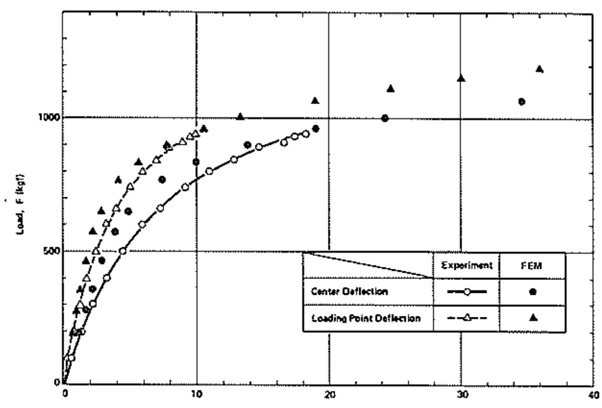

Fig. 10 Comparison of Measured and Calculated Load-Deflection Curve of Perforated Plate 1 at Room Temperature

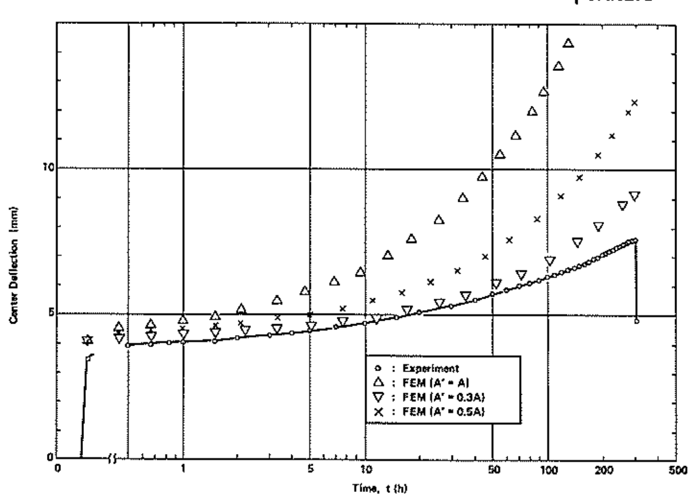

Fig. 11 Comparison of Measured and Calculated Time-dependent Response for Perforated Plate 5 at 600°C